17th Australasian Fluid Mechanics Conference
Auckland, New Zealand
5-9 December 2010

Early Transition of Separated and Reattaching Flows

M. C. Thompson

Fluids Laboratory for Aeronautical and Industrial Research
Department of Mechanical and Aerospace Engineering
Monash University, Clayton, Victoria 3800, Australia

Abstract

Experiments of a number of authors have indicated that the steady recirculation bubble that forms as the flow separates from the leading-edge corner of a long flat plate begins to flap at Reynolds numbers of less than 330. However, global stability analysis shows that the flow is absolutely *stable* at these Reynolds numbers, with both three-dimensional and the steady-to-unsteady transition occurring at Reynolds numbers of close to 400 or more. This situation is similar to the flow past a backward-facing step; in that case the separating shear layer undergoes flapping triggered by upstream flow noise exciting transition through transient exponential amplification of optimal perturbation modes. In this paper the optimal growth modes are studied to determine their role in triggering early transition to unsteady flow for a long flat plate. It is found that at $Re = 350$ the energy growth of the optimal disturbance is greater than 10^4. In practice, flow or acoustic noise, or rig vibration is not directly in the form of an optimal disturbance. As a model of a flow disturbance caused by plate vibration, the effect of suddenly moving the plate upwards with a very small but constant velocity is examined. It turns out such a perturbation excites the second most amplified optimal mode, leading to formation and shedding of shear-layer vortices some time later, similar to those observed experimentally.

Introduction

While global stability analysis has been highly successful in predicting the onset of flow transitions for many different types of flow problems, the Hopf bifurcation and three-dimensional transitions of a circular cylinder wake being prime examples (e.g., 6; 2), there are a number of other flows for which global stability predictions do not well describe the observed experimental behaviour. Classic example are 2D Poiseuille and Couette flows, which undergo turbulent transition even though stability analysis indicates absolute stability at observed transition Reynolds numbers. Another example is the flow over a backward-facing step. Barkley et al. (1) have shown that the initial absolute wake transition from the steady separated flow is through a three-dimensional steady transition rather than quasi-periodic flapping, which is commonly seen in experiments. The paper by Blackburn et al. (3) examines the problem in terms of transient growth of optimal initial spatial perturbation fields. It turns out that certain initial perturbations can undergo transient exponential amplifications as they are convected downstream leading to large-scale modification of the globally stable flow. These perturbations eventually die away and convect out of the system. Direct numerical simulations show that seeding the flow with low-level noise is sufficient to reproduce the flapping behaviour observed experimentally, in terms of both streamwise wavelength and mean frequency (3). This transition scenario also covers the smoothed backward-facing step (11) and stenotic flows (8; 4), i.e., flows through constrictions in pipes. In the latter case, remarkably high energy amplification factors of many orders of magnitude are observed when the blockage is substantial.

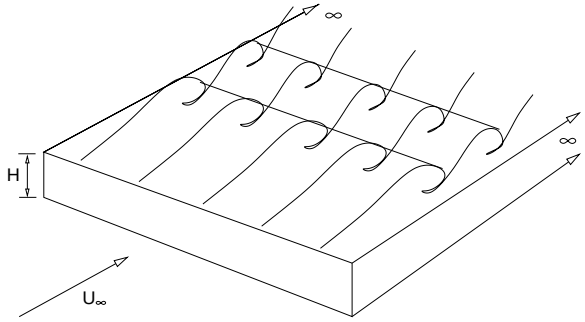

Figure 1: Problem setup: the plate is assumed semi-infinite in length and of infinite width. Above a certain Reynolds number the leading-edge separation bubble sheds quasi-periodic semi-discrete vortices.

Recent work (7) examines the boundary-layer flow over a smooth bump, which produces a downstream recirculation bubble. The particular geometry leads to flapping from the recirculation bubble above a certain Reynolds number, even in highly resolved low-noise numerical simulations. It seems that in this case global temporal modes undergo transition as a group with the frequencies separated by a fixed increment. This situation effectively leads to 'beating' between the temporal modes that correlates well with the observed flapping of the direct numerical simulations. Of interest, the global temporal modes resemble the evolved perturbation fields of the optimal perturbation modes, seemingly connecting the overall flow dynamics to both global and optimal growth modes. So it appears that flow dynamics at Reynolds numbers where the flow is absolutely unstable will be similar to the flow dynamics at subcritical Reynolds numbers where flapping is triggered by background noise.

The aim of the current paper is to examine the flow stability for a different geometry, that of a long flat plate with a square leading-edge. Relative to the geometries examined above, the flow near the leading-edge corner is more highly accelerated, but in general has similar characteristics. Both linear stability analysis and optimal perturbation mode analysis throw light on the flow dynamics, and indicate that the above discussed scenario for the cause of the flapping instability appears to be fairly generic.

Methodology

The flow under investigation is shown in figure 1. The geometry is a long flat plate with a square leading-edge. Ideally the plate is of (semi-)infinite length so that there is no feedback to the leading-edge shear layers as shed vortices pass the trailing edge. The plate geometry is two-dimensional. Above a Reynolds number of the order of $Re = U_\infty H/\nu = 100$, the flow separates from the leading edge corners and a separation bubble forms. Experiments indicate that at higher Reynolds numbers of $Re \sim 260$–330, a flapping instability of this recirculation zone leads to quasi-periodic shedding of vortex rollers. These vor-

tical structures appear to become three-dimensional soon after forming (13), although that is not the focus of this paper which concentrates on the initial two-dimensional flapping instability.

The flow is governed by the incompressible Navier-Stokes equations coupled with the continuity equation. From these the linearised Navier-Stokes equations can be extracted for the perturbation velocity $\mathbf{u}'(t,x,y,z)$ and pressure $p'(t,x,y,z)$. The linearised expansion is based on the two-dimensional steady base flow.

In this paper the focus is on transient growth of optimal disturbances, as previously examined for other flow geometries (e.g. (3; 9; 7; 5)). The analysis presented uses the approach described in (3) and so will only be briefly overviewed here. The aim is to determine the maximum energy growth of an initial perturbation for a chosen time period. This can be expressed as an eigenvalue problem in which the perturbation can be expressed in terms of a set of optimal modes which grow to different amplitudes over the chosen time interval. These growth amplitudes effectively represent the associated eigenvalues. Even though the base flow may be globally stable, the non-normality of the global modes can lead to massive amplification of perturbations, i.e., massive transient growth. The relative energy amplification (G - for growth) of an optimal mode is written as

$$G(\tau) = \frac{\mathcal{E}(t=\tau)}{\mathcal{E}(t=0)}, \qquad (1)$$

where $\mathcal{E}(t) = \frac{1}{2}\int (u'^2 + v'^2 + w'^2)\, d\mathcal{V}$ is the kinetic energy per unit mass in the perturbation velocity field at time t.

In practice, the determination of the optimal growth modes can proceed using the same time-stepping approach that can determine the linear stability of a steady base flow or the Floquet stability of time-periodic flows, i.e., integrating forward in time from a white noise perturbation field until only the dominant global modes remain. These can then be extracted based on a Krylov subspace approach using Arnoldi decomposition as described in Barkley and Henderson (2). For the optimal growth modes, the integration consists of two substeps: integrating the linear system forward in time until $t = \tau$; and then integrating the related adjoint linear system backwards in time, until $t = 0$. This can be repeated until the first few dominant optimal modes can be extracted to the desired accuracy.

The equations are discretised in space using the spectral-element approach. The current implementation of the software has been applied previously to various related problems, such as the wakes of cylinders (17; 19), spheres (18), tori (14; 15), and stenotic flows (8; 9). In terms of the current problem, the extension to the code to extract optimal growth modes has been validated by comparison with predictions from (5; 3). The current implementation is based on the description in (16).

This problem is relatively expensive in computational terms because of the sizeable regions with large velocity gradients requiring high resolution. The computational domain was rectangular with the mesh points concentrated towards the plate surfaces. The domain dimensions were: inflow length = $10H$, outflow length = $60H$, and the top and bottom boundaries located at $\pm 40H$, where H is the plate thickness. Spatial and temporal resolution and domain-size tests were performed to ensure that the predictions were reliable.

Results

Two-Dimensional Baseflow

Numerical simulations show that the flow evolves to a steady state for $Re \leq 450$. Below this and for $Re \geq 100$ a separation bubble forms at the top and bottom leading-edge corners. Thus the two-dimensional flow is temporally globally stable until at least $Re > 450$. However, experiments by various authors (12; 10; 13) indicate that separation bubble flapping begins to occur between $260 < Re < 330$; presumably the differences are caused by the background noise level. Figure 2 shows the variation of reattachment length with Reynolds number.

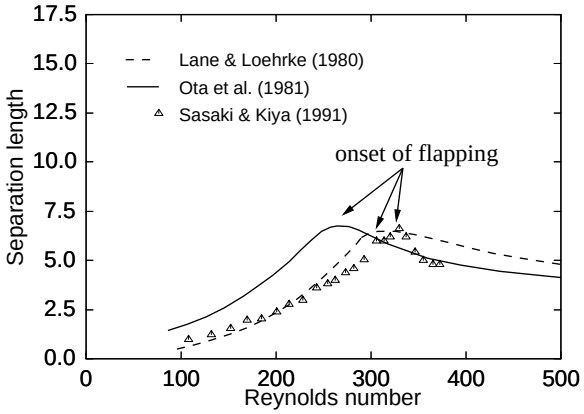

Figure 2: Reattachment length of the separation bubble as a function of Reynolds number from various experimental studies. Where the experimental curves turn over, the flow undergoes transition to unsteady shedding.

Absolute instability modes

A global linear stability analysis of the steady flow was performed to investigate the onset of three-dimensional flow. The results show that the flow undergoes a transition to three-dimensional steady flow at $Re \simeq 390$ for a spanwise wavelength of $\lambda \simeq 12H$. Like the backward-facing step, the initial transition is to a three-dimensional steady flow. Thus both 3D transition and the transition to unsteady flow occur at significantly higher Reynolds numbers than *effective* transition occurs in experiments.

Optimal growth solutions

The sensitivity of this flow to perturbations is well known. Apparently similar flows such as stenotic flow (4; 8), flow over a backward-facing step (3) and flow over a bump (11) show substantial energy amplification of optimal perturbation modes for moderate Reynolds numbers. Superficially at least these flows are similar in that there is an attached recirculation region bounded by a no-slip boundary on one side and a thin shear layer emanating from a separation point on the other. A small perturbation initially located near the separation point can undergo significant amplification as it advects along the shear layer.

The situation can be quantified by determining the set of perturbation modes that result in maximal growth over a given time interval τ. This can be done for different time intervals and different Reynolds numbers resulting in the energy amplification factor ($G(\tau, Re)$) of the dominant mode shown in figure 3. As the Reynolds number increases, for the same advection time, there is a rapid increase in the energy amplification of the dominant mode. For $Re = 450$, the energy growth is almost 7 orders of magnitude, indicating why it is difficult to obtain a steady flow at such Reynolds numbers in experiments, since the projections of background noise onto the optimal growth modes amplify to large levels as they are advected with the flow. The maximum growth occurs for larger values of τ as the Reynolds

number increases. This is consistent with the increase in separation bubble length with Reynolds number. The perturbation mode is amplified in the shear layer as it traverses the separation zone. Further downstream the mode decays, consistent with the fact that the flow is absolutely stable at these Reynolds numbers. Examining the maximum energy amplification with respect to τ at each Reynolds number indicates that maximum energy growth increases at 2.5 orders of magnitude for each Reynolds number increase of 100.

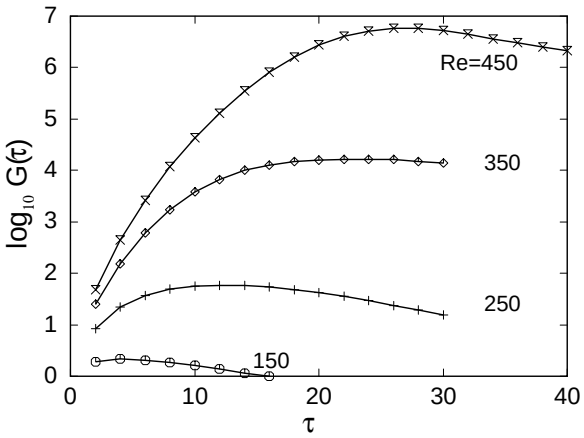

Figure 3: Energy amplification of the dominant mode as a function of non-dimensional time τ for various Reynolds numbers.

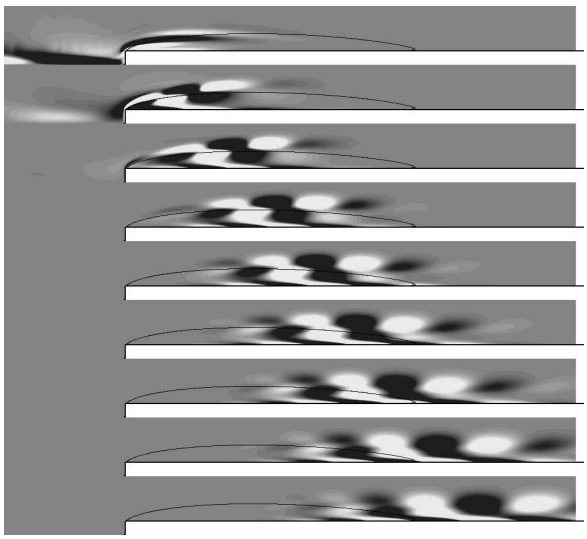

Figure 4: Evolution of the optimal initial disturbance with time for $\tau = 24$ and $Re = 350$. Times correspond to $t = 0, 3, 6, 9, 12, 15, 18, 21, 24$. The solid line indicates the separating streamline. Only the top half of the domain is shown to save space. The mode amplitude is maximum close to the leading-edge corner.

Figure 4 shows the evolution of the most amplified mode for $\tau = 24$ at $Re = 350$ in terms of perturbation vorticity. Note that the perturbation field grows along the separating streamline of the recirculation zone, similar to what would be expected for the Kelvin-Helmholtz shear-layer instability. The perturbation field begins to damp after it passes the end of the recirculation zone and is advected further downstream.

Nonlinear saturation

Figure 5 shows the evolved vorticity for the full flow field at $t = 15$ for an initial flow field consisting of the steady base flow perturbed by the optimal perturbation mode corresponding to $\tau = 24$ and $Re = 350$. The three cases considered are for maximum perturbation amplitudes of 0.3, 3 and 30% of the base velocity. These levels indicate the maximum percentage change to the base velocity field at any point over the entire flow domain. The lowest amplitude case effectively shows the induced linear perturbation to the otherwise steady vorticity field caused by the linear growth of the optimal perturbation mode as it advects downstream. The two higher amplitude cases show the nonlinear saturation of the perturbed flow. The main outcome of the nonlinear evolution of the optimal mode is, not surprisingly, the development of strong vortex rollers, as typically seen in experiments at this and higher Reynolds numbers (e.g., see references given in figure 2). These results also seem to be broadly consistent with the fact that experimentally it is not possible to observe a steady flow at Reynolds numbers higher than about 300–350.

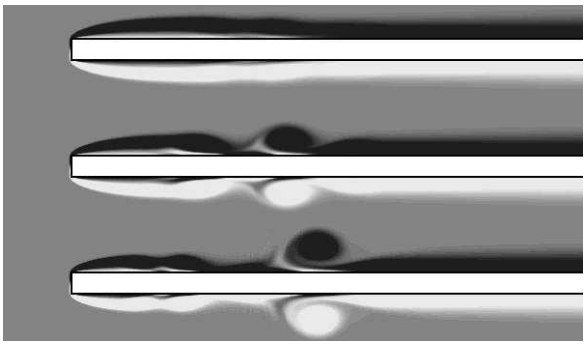

Figure 5: The effect of perturbing the flow with the optimal mode at different perturbation amplitudes. The vorticity field at $t = 15$ is shown for perturbation levels of 0.3%, 3% and 30%. The optimal mode used to perturb the flow corresponds to the dominant mode for $\tau = 24$ and $Re = 350$.

Growth of non-optimal disturbances

Real flows, of course, are subject to a variety of disturbances that may perturb the flow and substantially alter the behaviour of the flow from the ideal case. Examples include flow turbulence, acoustic perturbations and structural vibration, and flow-induced vibration. Another interesting generic perturbation to consider is the impulsive movement of the plate downwards at a constant, but very small, velocity, after the flow has reached a steady state. The obvious question is how is such a perturbation relates to the optimal perturbation modes previously examined?

Figure 6 shows the result if a multiple of the induced perturbation velocity field is added linearly to the steady base flow and the flow is evolved forward in time. This shows the vorticity field at $t = 15$ for $Re = 350$, for plate velocities of 0.0001, 0.001 and 0.01. Even for a perturbation velocity of 0.0001 the vorticity distribution at $t = 15$ still clearly shows the effect of perturbing the flow. This figure should be compared with figure 5 depicting the result for similar computations but using the dominant optimal mode to perturb the flow. Note that the non-alignment of vortices between the top and bottom surfaces of the plate in figure 6 is due to the symmetry characteristics of the imposed perturbation. In fact, the movement of the plate efficiently feeds energy into the second most dominant optimal mode, which has almost the same growth multiplier as the most dominant mode.

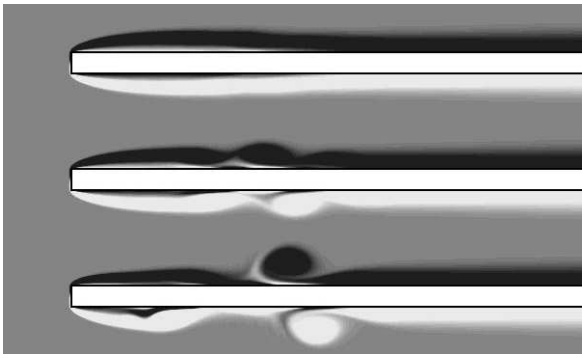

Figure 6: The effect of perturbing the flow by moving the plate at a constant velocity. The vorticity field at $t = 15$ is shown for plate velocities of 0.0001, 0.001 and 0.01.

Conclusions

The numerical simulations reported in this paper indicate that the flow dynamics of shear-layer flapping from a long flat plate are similar to those for the flow over a backward-facing step and a number of other related cases. The initial global transition appears to be a steady to steady three-dimensional transition around a Reynolds number of 390, with two-dimensional global temporal instability occurring at Reynolds numbers greater than 450. However, for this case and others, there is rapid amplification of optimal perturbation modes which effectively cause early transition in experiments, triggered by flow noise. At $Re = 350$, close to the very upper limit of the Reynolds number range for steady flow, the energy amplification is approximately 4 orders of magnitude. Moving the plate impulsively upwards with a very small velocity efficiently transfers energy into the second most dominant optimal mode leading to the characteristic shear-layer flapping as the perturbation advects downstream.

*

References

[1] Barkley, D., Gomes, M. G. M. and Henderson, R. D., Three-dimensional instability in flow over a backward-facing step, *J. Fluid Mech.*, **473**, 2002, 167–190.

[2] Barkley, D. and Henderson, R. D., Three-dimensional Floquet stability analysis of the wake of a circular cylinder, *J. Fluid Mech.*, **322**, 1996, 215–241.

[3] Blackburn, H. M., Barkley, D. and Sherwin, S. J., Convective instability and transient growth in flow over a backward-facing step, *J. Fluid Mech.*, **603**, 2008, 271–304.

[4] Blackburn, H. M., Sherwin, S. J. and Barkley, D., Convective instability and transient growth in steady and pulsatile stenotic flow, *J. Fluid Mech.*, **607**, 2008, 267–277.

[5] Butler, K. M. and Farrell, B. F., Three-dimensional optimal perturbations in viscous shear flow, *Phys. FLuids A*, **4**, 1992, 637–650.

[6] Dušek, J., Frauníe, P. and Le Gal, P., Local analysis of the onset of instability in shear flows, *Phys. Fluids*, **6**, 1994, 172–186.

[7] Ehrenstein, U. and Gallaire, F., Two-dimensional global low-frequency oscillations of a separating boundary layer flow, *J. Fluid Mech.*, **614**, 2008, 315–327.

[8] Griffith, M. D., Leweke, T., Thompson, M. C. and Hourigan, K., Steady inlet flow in stenotic geometries: Convective and absolute instabilities, *J. Fluid Mech.*, **616**, 2008, 111–133.

[9] Griffith, M. D., Thompson, M. C., T., L. and Hourigan, K., Convective instability in steady stenotic flow: optimal transient growth and experimental observation, *J. Fluid Mech.*, **655**, 2010, 504–514.

[10] Lane, J. C. and Loehrke, R. I., Leading-edge separation from a blunt plate at low Reynolds number, *ASME J. Fluid Eng.*, **102(11)**, 1980, 494–496.

[11] Marquet, O., Sipp, D., Chomaz, J.-M. and Jacquin, L., Amplifier and resonator dynamics of a low-Reynolds-number recirculation bubble in a global framework, *J. FLuid Mech.*, **605**, 2008, 429.

[12] Ota, T., Asano, Y. and Okawa, K., Reattachment length and transition of the separated flow over blunt flat plates, *Bulletin of the JSME*, **24(192)**, 1981, 941–947.

[13] Sasaki, K. and Kiya, M., Three-dimensional vortex structure in a leading-edge separation bubble at moderate Reynolds numbers, *J. Fluids Eng.*, **113**, 1991, 405–410.

[14] Sheard, G. J., Thompson, M. C. and Hourigan, K., From spheres to circular cylinders: the stability and flow structures of bluff ring wakes, *J. Fluid Mech.*, **492**, 2003, 147–180.

[15] Sheard, G. J., Thompson, M. C. and Hourigan, K., From spheres to circular cylinders: Non-axisymmetric transition in the flow past rings, *J. Fluid Mech.*, **506**, 2004, 45–78.

[16] Thompson, M. C., Hourigan, K., Cheung, A. and Leweke, T., Hydrodynamics of a particle impact on a wall, *Appl. Math. Model.*, **30**, 2006, 190–196.

[17] Thompson, M. C., Hourigan, K. and Sheridan, J., Three-dimensional instabilities in the wake of a circular cylinder, *Exp. Therm. Fluid Sci.*, **12**, 1996, 190–196.

[18] Thompson, M. C., Leweke, T. and Provansal, M., Kinematics and dynamics of sphere wake transition, *J. Fluids Struct.*, **15**, 2001, 575–585.

[19] Thompson, M. C., Leweke, T. and Williamson, C. H. K., The physical mechanism of transition in bluff body wakes, *J. Fluids Struct.*, **15**, 2001, 607–616.